International Journal of Bifurcation and Chaos, Vol. 25, No. 7 (2015) 1540004 (20 pages)

DOI: 10.1142/S0218127415400040

Strategies to Maximize Burst Lengths in Rhythmic Anti-Phase Activity of Networks with Reciprocal Inhibition

Amitabha Bose
Department of Mathematical Sciences,
New Jersey Institute of Technology,
Newark, NJ 07102, USA
bose@njit.edu

Jonathan E. Rubin
Department of Mathematics, University of Pittsburgh,
Pittsburgh, PA 15260, USA
jonrubin@pitt.edu

Received April 4, 2015

We consider repetitive activity patterns in which a pair of oscillators take turns becoming active, motivated by anti-phase bursting activity in neuronal networks. In our framework, when one unit is active, it inhibits the other, as occurs with inhibitory synaptic coupling of neurons; when the inhibition is strong enough, the inhibited unit is prevented from activating. We assume that the coupling resources available to each oscillator are constrained and allow each unit to select the amount of input that it provides to the other each time that it activates. In this setting, we investigate the strategies that each oscillator should utilize in order to maximize the number of spikes it can fire (or equivalently the amount of time it is active), corresponding to a burst of spikes in a neuron, before the other unit takes over. We derive a one-dimensional map whose fixed points correspond to periodic anti-phase bursting solutions. We introduce a novel numerical method to obtain the graph of this map and we extend the analysis to select solutions that achieve consistency between coupling resource use and recovery. Our analysis shows that corresponding to each fixed point of the map, there is actually an infinite number of related strategies that yield the same number of spikes per burst.

Keywords: Periodic activity; central pattern generator; discontinuous map; synaptic coupling.

1. Introduction

In the study of dynamical systems $x' = f(x, \alpha)$, $x \in \mathbb{R}^n$, $\alpha \in \mathbb{R}^m$, a fundamental problem is to prove the existence of solutions with particular properties, such as periodicity. Doing so commonly involves reducing the size of the phase space by exploiting differences in time scales or by deriving lower dimensional maps to obtain systems that are more tractable for analysis. Often, the dynamical system arises as a model for a specific application, and the application itself suggests a natural way to reduce the phase space. In this paper, motivated by a problem in neuroscience, we show how to derive and analyze a one-dimensional map that arises as a reduction of a larger system of equations. Using the map, we establish the existence of periodic solutions corresponding to anti-phase bursting of two reciprocally coupled neurons. The definition of the map arises naturally as a result of a specific modeling question regarding the optimization of burst length

that we shall describe below, and the approach would generalize to other systems featuring anti-phase oscillations, beyond the neuronal setting.

Neuronal networks are quite varied in the computations they can perform and the types of activity patterns they can display [Buzsaki, 2010]. For some networks, synchronization of the constituent elements is important for proper function [Singer, 1999; Butera *et al.*, 1999]. For others, the formation of distinct clusters of cells that oscillate out of phase with one another is a goal of the network [Terman & Wang, 1995; Chandrasekaran *et al.*, 1999; Huntsman *et al.*, 1999; Rubin & Terman, 2000]. In the case of winner-take-all networks, it is a group of cells that ends up dominating the network activity, while some other group of cells remains suppressed [Ermentrout, 1992; Kaski & Kohonen, 1994]. In all of these cases, the network structure and the properties of the interactions among its elements combine to determine the particular forms of activity that emerge. In this work, we study how certain patterns of neuronal interactions can, in some sense, optimize particular forms of anti-phase firing.

A variety of works have applied optimization methods to consider the ideal form of external stimulation to alter the activity of a neuronal network in some particular way [Feng *et al.*, 2007; Nabi *et al.*, 2013; Popovych & Tass, 2014]. Optimization approaches to study the natural function of neuronal networks have received less attention but offer the potential to yield insights about why particular properties are present in these systems [Forger & Paydarfar, 2004; Moehlis *et al.*, 2006; Wang *et al.*, 2011; Forger *et al.*, 2011; Clay *et al.*, 2012]. For example, in recent work, we identified patterns of synaptic inputs, subject to various constraints on the total synaptic resources available, that would maximize firing of a postsynaptic neuron, and we showed how the optimal patterns depend on the intrinsic dynamic properties of the postsynaptic target [Wang *et al.*, 2011]. In that paper, however, we assumed that the firing times of the presynaptic neuron could be selected arbitrarily.

In this work, we move beyond that assumption to consider optimization in a pair of model neurons coupled reciprocally with synaptic inhibition that take turns firing. Here, the firing times of each active neuron can be easily computed from the dynamics of the neuronal model, while the amount of synaptic conductance imparted by the active neuron's spikes and the suppressed cell's dynamics determine the amount of time before the neurons switch roles. We assume that the maximal synaptic conductance induced by each spike is free to be optimized, subject to certain constraints including a finite limit on the total resources available within an active period. Because the total amount of synaptic resources is finite, the active cell will ultimately use all of its resources and the other cell can become active, thereby switching their two roles. In this setting, we analyze activity patterns in which the neurons take turns firing one or more successive spikes, and we determine patterns of synaptic conductance amplitudes that maximize the number of spikes each neuron fires when active. Because the time it takes a neuron to fire each spike (after its first) is fixed in our model, maximizing spike number corresponds to maximizing the amount of time that each neuron is active. We will show that there are an infinite number of strategies that cells can employ to maximize the number of spikes they can fire, but that these strategies are all related, leading to the same number of spikes independent of the strategy.

Mathematically, the main focus of this paper is the derivation, analysis and numerical computation of a one-dimensional map, $\Pi(r)$. This map, from an interval into itself, characterizes how the last synaptic input a cell receives at the end of its silent period is related to the last synaptic input that it will be able to provide at the end of its own active period. Fixed points of the map correspond to periodic anti-phase bursting solutions of the two cell network. The map turns out to be piecewise differentiable and offers the possibility for multistability of periodic solutions. We also derive a novel numerical method using XPPAUT [Ermentrout, 2002] to numerically determine the graph of $\Pi(r)$. The idea of this method is to solve a boundary value problem that simultaneously characterizes certain features of the spiking periods both before and after a transition in which the silent and active neurons switch roles.

Our line of analysis is motivated by several considerations. Our approach may be useful for gaining insights into the patterns of short-term synaptic depression or facilitation that are observed experimentally. Indeed, experiments have described a wide variety of patterns of weakening or strengthening of synaptic currents or potentials over successive spikes [Zucker & Regehr, 2002]. It is known that these patterns result from probabilistic synaptic release and other molecular-level details of the

synaptic transmission process, but why particular synaptic connections exhibit corresponding release properties is less well understood (but see [Fortune & Rose, 2001; Rosenbaum *et al.*, 2012, 2013] and the references therein). Our work is also motivated by the study of central pattern generating (CPG) networks, which can oscillate without any rhythmic sensory input. CPGs control vital motor networks associated with critical functions, such as heartbeat [Masino & Calabrese, 2001], breathing [Smith *et al.*, 2009] and digestion [Marder & Bucher, 2007], and often include groups of neurons that oscillate out of phase with one another. In the case of just two cells or clusters, this can lead to half-center oscillations where, at any moment in time, one of the cells (clusters) is active, while the other is silent [Skinner *et al.*, 1994]. It is possible that short term synaptic properties constitute an important part of CPG function, contributing to the ability of CPGs to flexibly adjust frequencies and relative phase durations in response to different metabolic or top-down demands [Marder *et al.*, 2005; Mitchell & Johnson, 2003; Morris *et al.*, 2003]. In this context, our analysis is aimed at broadening our understanding of how variations in synaptic conductances across successive spikes could contribute to the characteristics of CPG activity patterns.

The paper is organized as follows. In Sec. 2, we introduce the equations associated with the integrate- and fire-model and coupling between cells that we utilize throughout the paper; an Appendix presents a more general framework to which the ideas in this paper will generalize. In Secs. 3.1 and 3.2, we derive the map $\Pi(r)$. In Sec. 3.3, we present the boundary value problem that we solved in XPPAUT to numerically compute the map. Section 3.4 includes to the recovery of synaptic resources, while Sec. 3.5 focuses on the dynamics of $\Pi(r)$ and on strategies for creating optimal periodic solutions. Finally in Sec. 3.6, we present a different direct proof of the existence of anti-phase spiking solutions, which is of interest in its own right. We conclude with a brief discussion in Sec. 4.

2. Model

Consider a pair of oscillators coupled through mutually inhibitory synapses. Assume that each oscillator is able to (i) fire a series of spikes (burst), and (ii) determine the strength with which it inhibits the other oscillator each time it fires a spike. Within the inhibitory two-oscillator network, we refer to the unit that most recently reached threshold as *active* and the other as *silent*. We seek to analyze solutions in which the oscillators take turns being active, with each oscillator firing some number of consecutive times before the other one takes over.

Although the analysis in this paper can be cast in a quite general framework (see Appendix), all results in this paper will be derived for the integrate-and fire-neuron model. The model for an isolated neuron is given by

$$v' = I - v, \tag{1}$$

where v denotes the voltage of the cell. When the voltage v reaches a threshold, here set to $v = 1$, the cell fires a spike. The voltage is then instantaneously reset to $v = 0$. That is, the voltage reset condition is

$$v(t) = 1 \Rightarrow v(t^+) = 0. \tag{2}$$

Note that in the absence of a threshold, $v = I$ is a stable fixed point for (1). Thus the neuron will fire periodically if $I > 1$, otherwise it will not. We will henceforth assume that $I > 1$, in which case it is easy to calculate that the period of the neuron is given by $T = \ln(\frac{I}{I-1})$.

When two neurons are reciprocally coupled by inhibition, the equations governing the dynamics of each cell are given by

$$v_i' = I - v_i - g_j(v_i - E), \quad g_i' = -\beta g_i, \tag{3}$$

where $i = 1, 2$ and $i \neq j$. Here g_i refers to the conductance of each synapse and E is the synaptic reversal potential with $E < 0$. We assume that after spikes of cell j, Eq. (2) holds and the synaptic variable g_j is reset to $g_j + k_n$, where $k_n > 0$ for spikes $n = 1, 2, 3, \ldots$. Note that the term g_j shows up in the equation for v_i, corresponding to the fact that cell j inhibits cell i. For analytical tractability, we make the additional assumption that when cell i is active, after its first passage from reset ($v = 0$) to threshold ($v = 1$), $g_j = 0$, such that its voltage equation reduces to (1). With this assumption, the time between all spikes after a brief transient is fixed, such that maximizing the number of spikes fired corresponds to maximizing active phase duration.

Biologically, increases in synaptic conductance result from neurotransmitter release by the spiking cell, and individual cells have constrained neurotransmitter supplies to work with, although these are gradually replenished. Suppose that when a

neuron becomes active, it has synaptic resources $M > 0$, meaning that it has enough neurotransmitter available to cause the synaptic conductance to rise within a specified time (to be determined below) by an amount M. When an active cell j fires its nth spike and g_j is increased by k_n, its remaining available synaptic resources are decreased by an amount k_n correspondingly. To keep track of the remaining amount of synaptic resources after the nth spike, define $R_n = M - \Sigma_{l=1}^{n} k_l$, with $R_0 = M$. In the later parts of the paper, starting from Sec. 3.4, we add realism to the model by assuming that a cell recovers its synaptic resources when it is silent and that there are specific dynamics associated with this process. Specifically, we assume that the synaptic resources of cell are recovered when it is in the silent phase according to the equation

$$R' = \rho(S - R) \tag{4}$$

for some $S > 0$ and $\rho > 0$.

Assuming that two cells have identical synaptic resource recovery dynamics, an anti-phase bursting periodic orbit of the two cells c_1 and c_2 would consist of c_1 being active and firing N spikes while c_2 is silent, followed by c_2 firing N spikes while c_1 is active, and so on, with both cells giving the same synaptic kicks (i.e. releasing the same amount of synaptic resources) on their corresponding spikes. For any $N > 0$, by choosing the synaptic kick sizes appropriately, we can always arrange for $R_N = 0$. When this occurs, we say that the periodic orbit is *synaptically exhaustive*. Further if N is maximized, as described below, we say that the oscillation is *optimally periodic*.

Let τ denote the period of one full cycle of the anti-phase burst where each cell has completed one active phase. For the sake of argument, let us assume that c_1 is active first, on $(0, \tau/2)$, while c_2 is active second, on $(\tau/2, \tau)$. For the existence of a synaptically exhaustive, optimally periodic orbit that uses synaptic resources M within each active phase, the following must hold:

(a) for c_1 there exists a set of spike times $\{t_i\} \in (0, \tau/2)$ and a synaptic strategy with kick sizes $\{k_i\}$, $i = 1, \ldots, N$ such that $R_0 = M$, $R_N = 0$ and N is maximized, and
(b) for c_2, the period τ, which is determined by the chosen synaptic strategy in (a), satisfies the consistency condition $R(0) = 0$ and $R(\tau/2) = M$.

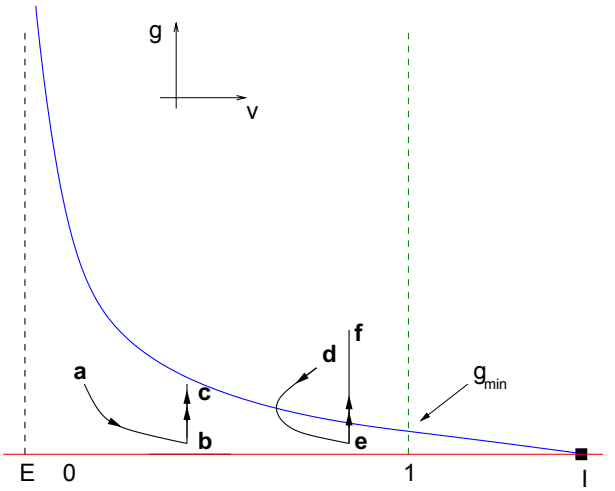

Fig. 1. The v–g phase plane. The v-(blue) and g-(red) nullclines are shown together with representative trajectories. Single arrows denote the flow, while double arrows denote the instantaneous reset due to synaptic input. The size of the particular synaptic input determines the vertical distance through which a trajectory is reset.

A similar set of statements applies over the interval $(\tau/2, \tau)$. We will show that there are an infinite number of synaptic strategies that lead to a synaptically exhaustive, optimally periodic solution.

Much of the analysis will be done in the v–g phase plane; see Fig. 1. The v-nullcline is the set of points $\{(v, g) : g = (I - v)/(v - E)\}$ which is a concave up decreasing graph (blue curve) with a vertical asymptote at $v = E$ (black dashed line). This nullcline intersects the threshold $v = 1$ (green dashed line) at a value

$$g_{\min} = \frac{I - 1}{1 - E}. \tag{5}$$

The g-nullcline is simply the v-axis (red line). When the threshold and synaptic kicks are ignored, the intersection $(I, 0)$ of the v- and g-nullclines is an asymptotically stable fixed point for the flow given by Eq. (3), for $i = 1, 2$. In Fig. 1, we show two typical trajectories and the effect of synaptic input. The trajectory starting at point **a** initially lies below the v-nullcline and thus flows to the right. At point **b**, it receives a synaptic input and is reset vertically to point **c**. Depending on the size of the input, the reset point may be above the v-nullcline, as is the case with the trajectory starting at point **d**. Initially, this trajectory lies above the v-nullcline, so it flows left, crosses below the v-nullcline and then flows right to point **e**. There, it receives a large synaptic kick placing it at point **f** above the v-nullcline.

3. Results

3.1. *Existence of a stable suppressed solution*

An anti-phase bursting solution will consist of the active cell firing a number of times, while the other is silent, followed by the two cells switching roles. During the time when one cell is firing, the other is suppressed. We first prove that if we ignore the upper bound M on the total synaptic conductance, then there exists a stable suppressed solution. This is equivalent to finding conditions under which one cell, say c_1, fires periodically, while the second cell, c_2, lies below threshold for all time. This is also equivalent to simply considering a feedforward network in which c_1 inhibits c_2.

We begin by proving a set of results that ignores the spiking threshold $v = 1$. Fix $I > 1$, $E < 0$ and recall that T is the intrinsic period of an isolated neuron. The following proposition proves the existence of a suppressed solution.

Proposition 1. *For each $k > 0$, there exist v^* and g^* such that $(v^*, g^*) \cdot T^- = (v^*, g^* - k)$.*

Proof. Solve the equation $g'(t) = -\beta g(t)$ to obtain $g(T^-) = g(0)e^{-\beta T^-}$. We use the periodicity condition $g(T^-) = g(0) - k$ to find that $g(0) = k/(1 - e^{-\beta T^-})$ and set $g^* = g(0)$, so

$$g^* = \frac{k}{1 - e^{-\beta T^-}}. \tag{6}$$

Now we ignore the $v = 1$ threshold in order to determine v^*. First, we solve the equation $v' = I - v - g(v - E)$ using the integrating factor $\exp(t - (g(0)/\beta)e^{-\beta t})$, which we will denote as $h(t, g)$. We find that $v(t)h(t, g) - v(0)h(t, 0) = \int_0^t (I + g(s)E)h(s, g)\mathrm{d}s$. Now apply the periodicity condition $v(0) = v(T^-) = v^*$, and set $g(0) = g^*$ to yield $v^*(h(T^-, g^*) - e^{-g^*/\beta}) = \int_0^{T^-} (I + g^* e^{-\beta s} E)h(s, g^*)ds$. It follows that

$$v^* = \frac{\displaystyle\int_0^{T^-} (I + g^* e^{-\beta s} E)h(s, g^*)ds}{h(T^-, g^*) - e^{-g^*/\beta}}. \tag{7}$$

We can see that g^* and v^* satisfy our requirements and have been uniquely determined based on our fixed value of k. ■

Note that as $k \to 0$, $g^* \to 0$ and $v^* \to I > 1$. However, since $v = 1$ is the threshold, we are interested in values where $v^* \leq 1$ and $g^* > g_{\min}$. From (5) and (6), the latter inequality places a restriction on the minimum value of the inhibitory kick as

$$k_{\min} > (1 - e^{-\beta T}) \left(\frac{I - 1}{1 - E} \right).$$

We let $\mathbf{\Lambda}(k)$ denote the trajectory found in Proposition 1 with initial condition (v^*, g^*). When $k > k_{\min}$, $\mathbf{\Lambda}(k)$ is the trajectory of the suppressed cell in the feed-forward network of c_1 inhibiting c_2. In order to later find an optimally periodic solution, we are interested in finding a suppressed trajectory that minimizes the necessary kick size. It turns out that this corresponds to the suppressed trajectory that has $v^* = 1^-$.

Corollary 1. *There exist $k^* > k_{\min}$ and $g^*_{k^*} > 0$ such that $(1^-, g^*_{k^*}) \cdot T^- = (1^-, g^*_{k^*} - k^*)$.*

Proof. Define a map $f : [g_{\min}, \infty) \to [0, \infty)$ given by $f(g) = t_g$, where t_g is the time it takes the trajectory originating at the point $(1^-, g)$ in the phase plane to reach threshold. Note that $f(g_{\min}) = 0$. Every trajectory starting at $(1^-, g)$ for $g > g_{\min}$ has $v' < 0$ and $g' < 0$. Thus such a trajectory moves down and into the region with $v < 1$. It crosses the v-nullcline, after which $v' > 0$, and eventually reaches the threshold at $v = 1$. All this while, $g' = -\beta g < 0$. Thus if we choose $g_1 = g_{\min} e^{\beta T}$, then the trajectory starting at $(1^-, g_1)$ will be more than time T away from threshold. This is because by uniqueness of solutions, at time T, the trajectory will lie to the left of $(1, g_{\min})$ on $\{g = g_{\min}\}$. Therefore by the intermediate value theorem, there exists a value $g^*_{k^*} \in (g_{\min}, g_1)$ such that $f(g^*_{k^*}) = T$. Using Proposition 1, we now define k^* to satisfy $g^*_{k^*} \cdot T = g^*_{k^*} - k^*$. ■

Using the notation defined above, the trajectory identified in Corollary 1 can be labeled as $\mathbf{\Lambda}(k^*)$. The maximum value along $v = 1$ for this trajectory is $g^*_{k^*}$ and the minimum value is $g_0 = g^*_{k^*} e^{-\beta T}$ (Fig. 2). Using this notation, note that k^* satisfies $k^* = g_0(e^{\beta T} - 1)$ or, alternatively, $k^* = g^*_{k^*}(1 - e^{-\beta T})$.

We next prove that in the feed-forward network of c_1 inhibiting c_2, the suppressed solution is stable. We define a map $\mu(v, g)$ which takes an initial iterate $(v_2, g_2) = (v(0), g(0))$ and returns a new value $(v_2, g_2) = (v(T^+), g(T^+))$, where $g(T^+) = g(T^-) + k^*$. Each time the active cell fires, the map

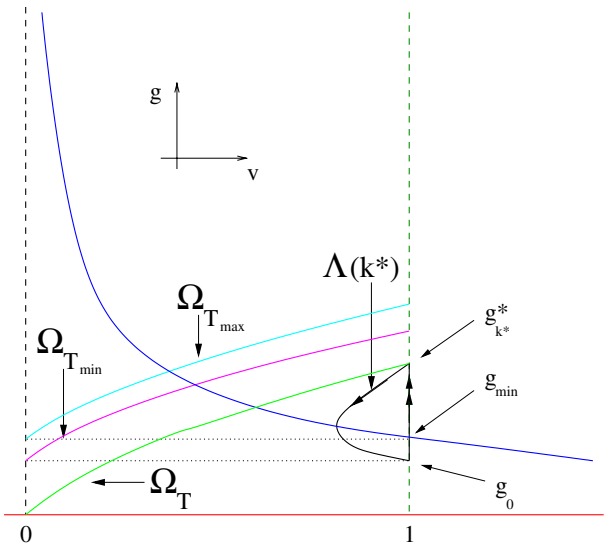

Fig. 2. Objects within the v–g phase plane that are used to construct an optimally periodic solution. The suppressed trajectory $\Lambda(k^*)$ that travels between $g^*_{k^*}$ and g_0 is shown in black. The curves Ω_T (green), $\Omega_{T_{\min}}$ (magenta) and $\Omega_{T_{\max}}$ (cyan) represent points that lie at time T, $T_{\min}$ and $T_{\max}$ respectively away from threshold.

μ marks the location of the suppressed trajectory after it has been reset. Note that (v^*, g^*) is a fixed point of μ.

Proposition 2. *The value (v^*, g^*) is an asymptotically stable fixed point of the map μ.*

Proof. We first determine that g^* is attracting, since it is independent of v. Recall that $g^* - k^* = g^* e^{-\beta T^-}$. Let $g(0) = g^* + \delta$. Then $g(T^-) = g^* e^{-\beta T^-} + \delta e^{-\beta T^-} = g^* - k^* + \delta e^{-\beta T^-}$. Since $0 < e^{-\beta T^-} < 1$, $g(T^-) < g^* - k^* + \delta$ if $\delta > 0$, and $g(T^-) > g^* - k^* + \delta$ if $\delta < 0$. This implies that $g(T) < g^* + \delta$ if $\delta > 0$, and $g(T) > g^* + \delta$ if $\delta < 0$. Thus, after each kick, the solution is closer to g^*. Hence, g^* must be attracting.

Next for simplicity, let

$$F(t) = \int_0^t (I + g^* e^{-\beta s} E) h(s, g^*) ds.$$

Then

$$v^* = \frac{F(T)}{h(T, g^*) - h(0, g^*)}. \tag{8}$$

Using this notation, we can write

$$v(T^-) = \frac{v(0) h(0, g^*)}{h(T^-, g^*)} + \frac{F(T^-)}{h(T^-, g^*)}.$$

It is clear that using $v(0) = v^*$ and (8), we obtain $v(T^-) = v^*$, as expected. Now let $v(0) = v^* + \delta$. Then $v(T^-) = \frac{(v^*+\delta)h(0,g^*)}{h(T^-,g^*)} + \frac{F(T^-)}{h(T^-,g^*)}$. Using (8), we can simplify this to

$$v(T^-) = v^* + \delta \left(\frac{h(0, g^*)}{h(T^-, g^*)} \right).$$

We will now show that $h(0, g^*) < h(T^-, g^*)$, where $h(T^-, g^*) = \exp(T^- - (g^*/\beta) e^{-\beta T^-})$ and $h(0, g^*) = e^{-g^*/\beta}$. $e^{T^-} > 1$ since $T > 0$, and $e^{-\beta T^-} < 1$ since $\beta > 0$. So $\frac{g^*}{\beta} > \frac{g^*}{\beta} e^{-\beta T^-}$, and hence, $e^{-g^*/\beta} < e^{-(g^*/\beta) e^{-\beta T^-}}$. Thus, $h(0, g^*) < h(T^-, g^*)$, as desired. It follows that if $\delta > 0$, then $v(T^-) < v^* + \delta$, and if $\delta < 0$, then $v(T^-) > v^* + \delta$. Thus, after time T, the solution has moved closer to v^*. Hence, v^* must be attracting, allowing us to conclude that the fixed point (v^*, g^*) is attracting. ■

Remark 3.1

(1) It now follows that the trajectory $\mathbf{\Lambda}(k^*)$ must be contained as part of an attracting periodic orbit corresponding to the suppressed solution of the two cell c_1, c_2 network.
(2) There are other suppressed solutions that can exist. Suppose a suppressed cell starts along $v = 1$ with $\tilde{g} > g_{\min}$, a time $2T$ away from threshold. Then the active cell would need to inhibit the suppressed cell every other cycle to maintain suppression. However, it is easy to see that the needed kick size in this case is larger than $2k^*$. Thus this strategy would not lead to an optimal periodic solution.
(3) Note that if the suppressed cell lies on $\mathbf{\Lambda}(k^*)$ at $(1^-, g_0)$, then k^* is the minimum kick size needed to maintain suppression.

3.2. *The anti-phase bursting solution*

Consider now a mutually coupled network of two cells, c_1 and c_2. The idea behind finding an anti-phase bursting solution is that while one cell is firing periodically, the other cell lies along the trajectory $\mathbf{\Lambda}(k^*)$. Once the synaptic resources have been sufficiently depleted, the silent cell will begin firing and the formerly active cell will now become silent. Because μ has an attracting fixed point associated with the trajectory $\mathbf{\Lambda}(k^*)$, the newly silent cell will be attracted towards $\mathbf{\Lambda}(k^*)$, which it will follow until resource depletion allows the process to repeat. In fact, as we will show below, by choosing appropriate synaptic kick sizes, we can place the

newly suppressed trajectory directly onto $\mathbf{\Lambda}(k^*)$. We assume for now that each cell has synaptic resources M available, for some fixed $M > 0$, that these are diminished by each synaptic release while the cell is spiking, and these are fully replenished while the cell is silent. We will return to the issue of recovery of resources later, in Sec. 3.4.

We introduce some additional notation and definitions. Consider the line segment with $v = 1$ lying between $g = 0$ and $g_0 = g^*_{k^*}e^{-\beta T}$. Flow this line segment backward for time τ. This yields a curve that we denote Ω_τ. Note that any initial condition that lies to the left of Ω_τ lies more than time τ away from threshold, while those that lie to the right of it are less than time τ away. The curve Ω_τ is a monotone increasing curve that shifts up with increasing β. When $\tau = T$, the value of the intrinsic period of an uncoupled cell, then Ω_T intersects the v-axis at $v = 0$ and the threshold $v = 1$ at the point $g = g^*_{k^*}$. Numerical examples of Ω_τ for pairs of τ values are shown for two different β values in Fig. 3.

The following two lemmas are general results that essentially follow from uniqueness of solutions, which prevents distinct trajectories from crossing.

Lemma 1. *If* $v_1(0) = v_2(0)$ *and* $g_1(0) < g_2(0)$, *then the trajectory with initial conditions* $(v_1(0), g_1(0))$ *reaches threshold before the trajectory with initial conditions* $(v_2(0), g_2(0))$.

Lemma 2. *If* $v_1(0) > v_2(0)$ *and* $g_1(0) = g_2(0)$, *then the trajectory with initial conditions* $(v_1(0), g_1(0))$ *reaches threshold before the trajectory with initial conditions* $(v_2(0), g_2(0))$.

Let $T_{\max}$ and $T_{\min}$ be the respective times it takes trajectories with initial conditions $(0, g_{\min})$ and $(0, g_0)$ to reach threshold. Note that $T_{\max} > T_{\min}$ as a consequence of Lemma 1. Similarly to Ω_T, we define the curves $\Omega_{T_{\min}}$ and $\Omega_{T_{\max}}$ such that initial conditions lying on these curves are times $T_{\min}$ and $T_{\max}$ away from threshold, respectively; see Fig. 2. Denote by $\hat{g}$ the value of g at which $\Omega_{T_{\max}}$ intersects $v = 1$. Note that $\hat{g} > g^*_{k^*}$. Fix $M > 2\hat{g}$. For reasons that will become clear below, this choice guarantees that each cell in the anti-phase solution fires at least three spikes per burst. Assume that the active cell delivers a sequence of synaptic kicks $\{k_i\}$ to the silent cell. Recall the definition of $R_n = M - \Sigma_{i=1}^n k_i$, with $R_0 = M$, which measures the remaining amount of synaptic resources after the nth spike. Observe that for any j, if $R_j > k^*$, then the active cell has sufficient synaptic resources

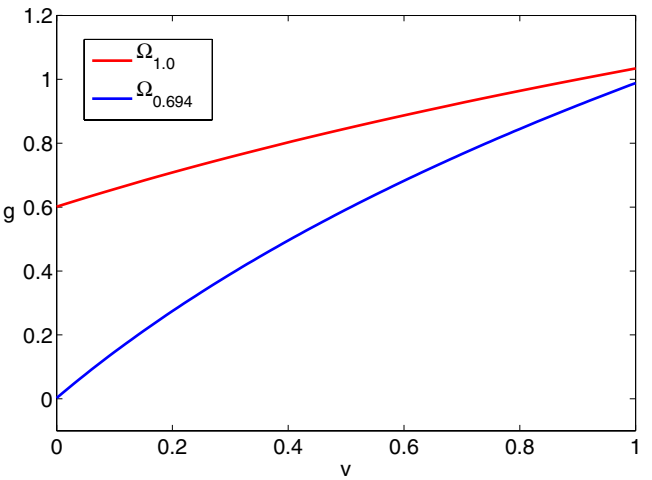

(a)

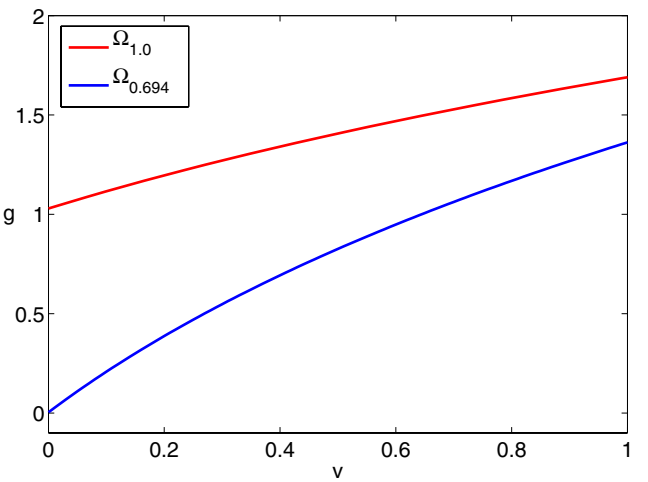

(b)

Fig. 3. Numerical examples of $\Omega_{0.694}$ and $\Omega_{1.0}$ for (a) $\beta = 0.2$ and (b) $\beta = 1.0$. The intrinsic period of an uncoupled neuron is $T = 0.694$ for the parameters chosen and correspondingly the curve $\Omega_{0.694}$ passes through the origin. Note that the two panels have different vertical scales. As β grows, both between these values and above 1.0, g decays faster and thus Ω_τ increases for each fixed τ.

left to suppress the silent cell for at least one more cycle, if the silent cell is on $\Lambda(k^*)$.

For each $r \in [0, k^*]$ we will determine unique values $k_1(r)$, $k_2(r)$ and $m \geq 0$ such that $M = k_1(r) + k_2(r) + mk^* + r$. The idea is the following. Assume that the silent cell has $v = 1^-$ when the active cell fires what will be its final spike of the cycle, providing the silent cell with a synaptic input of size $r = r_{\text{last}}$, such that the input pattern is synaptically exhaustive. As a result, the currently silent cell jumps to $(1^-, g_0 + r_{\text{last}})$ while the

currently active cell is reset to $(0, 0)$. Let δr be the time it takes the trajectory from $(1^-, g_0 + r_{\text{last}})$ to reach threshold. Note that if $r_{\text{last}} \in (0, g_{\min} - g_0)$, then $\delta r = 0$ and the trajectory immediately reaches threshold. If $r_{\text{last}} \in (g_{\min} - g_0, k^*)$, then $\delta r > 0$. Once the silent cell reaches threshold, it becomes the active cell and inhibits the other cell. It then will use two cycles and associated synaptic kicks $k_1(r)$ and $k_2(r)$ to position the newly suppressed, now silent, cell onto $\mathbf{\Lambda}(k^*)$. From this point on, the active cell delivers kicks of size k^*, keeping the silent cell on $\mathbf{\Lambda}(k^*)$. So long as $R_j > k^*$, the active cell can fire a $(j+1)$th spike that will maintain suppression of the silent cell. By definition there exists an m such that $R_j > k^*$ for $j = 0, 1, \ldots, m+1$, $R_{m+2} < k^*$ and $R_{m+3} = 0$. We call $R_{m+2} = r_{\text{new}}$. If $r_{\text{new}} = r_{\text{last}}$ then the currently silent cell receives its last synaptic input of exactly the same size as the last synaptic input of the previously silent cell. This matching corresponds to a periodic solution where each cell fires $m+3$ spikes in the anti-phase burst; if $k_1(r)$ and $k_2(r)$ are chosen appropriately, then for the resulting m, $m+3$ is the maximal number of spikes a cell can fire for given synaptic resources M, at least locally within the space of strategies (see Sec. 4), such that we call the pattern optimally periodic.

This construction leads to the definition of a map

$$\Pi(r) = M - k_1(r) - k_2(r) - mk^* \tag{9}$$

that takes the r value (the last synaptic kick size) of the currently silent cell and determines the r value that the newly silent cell will ultimately receive at the end of its suppressed phase. The map is defined based on the flow from the initial condition with the currently silent cell located at $(1^-, g_0 + r)$ and the currently active cell located at $(0, 0)$. After the currently silent cell has fired, it will be reset to a value $(0, g_r)$ where $g_r \in [g_0, g_{\min}]$. For each r, we denote by $T(r)$ the time it takes a cell starting at $(0, g_r)$ to reach threshold. As we will show below, $T(r)$ plays an important role in determining the dynamics of the map $\Pi(r)$.

Theorem 1. *Suppose that $M - k_1(r) - k_2(r) \geq 0$ for all $r \in [0, k^*)$. $\Pi(r) : [0, k^*) \to [0, k^*)$ is a piecewise continuous map that is differentiable at each point of continuity. It is a decreasing function on each interval where it is continuous within $(0, g_{\min} - g_0)$ and, assuming that $T'(r)$ is sufficiently small or that $dk_1(r)/dr$ is bounded away from 0 as β increases, it is decreasing where it is continuous within $(g_{\min} - g_0, k^*)$ as well. The map increases from 0 to k^* at all points of discontinuity and has at least one fixed point, corresponding to a synaptically exhaustive, optimally periodic solution of system (3) with the reset condition (2).*

Proof. There are two distinct intervals to consider depending on the value of r. First choose $r \in [0, g_{\min} - g_0)$. In the construction of $\Pi(r)$, we start at the moment that the currently silent cell receives its final input, of size r, and the active cell is at $(v, g) = (0, 0)$. In this case, upon receipt of the final input, the currently silent cell lies below the v-nullcline, such that $\delta r = 0$ and the cell reaches threshold immediately. It will then become active, fire and be reset to $(0, g_0 + r)$ in phase space. Define the input to the other cell, which started at $(0, 0)$, as $k_1(r) = (g_0 + r)^+$. This input places the newly silent cell at the same voltage as the newly active cell but at an infinitesimally larger g value. The newly active cell will then evolve and reach the threshold $v = 1$ at some time $T(r) \in (T_{\min}, T_{\max})$ with the silent cell trailing it to $v = 1^-$. Note that $dT(r)/dr > 0$ on the interval $[0, g_{\min} - g_0)$; see Fig. 4. Next choose

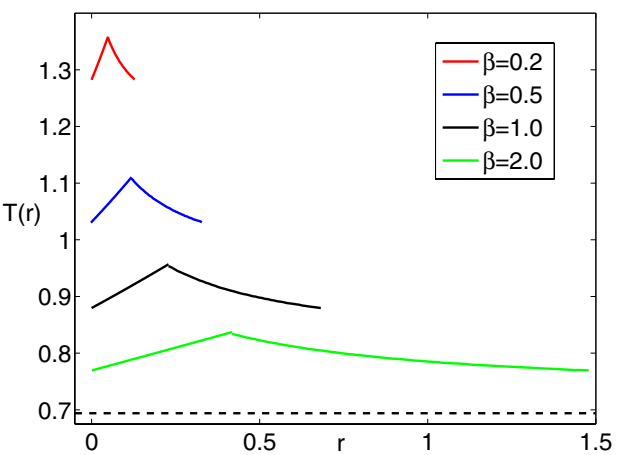

Fig. 4. Numerical examples of $T(r)$ for $E = -0.1$, $I = 2$ and various values of β. On the interval $(0, g_{\min} - g_0)$, $T(r)$ is an increasing function of r, while it is decreasing on the remainder of the interval for each fixed β. For each of the curves shown, the minimum value equals $T_{\min}$ and is attained at the endpoints of the interval. The maximum value, which equals $T_{\max}$, occurs at $r = g_{\min} - g_0$. These values depend on β. As β increases, g decays faster, which allows v to grow from 0 to 1 faster, and hence $T(r)$ decreases. Similarly, the value g_0 decreases (and $g^*_{k^*}$ increases) as β increases, whereas $g_{\min}$ stays fixed at the value given in (5). The dashed black line is the time of passage T from $v = 0$ to $v = 1$ with $g = 0$ which is a firm lower bound on $T(r)$ for all β.

$k_2(r) = g^*_{k^*} - (g_0 + r)\exp(-\beta T(r))$. When the active cell fires and provides this input to the suppressed cell, the suppressed cell is kicked to $(1^-, g^*_{k^*})$, at the maximal location on $\mathbf{\Lambda}(k^*)$, and the active cell is reset to $(0, 0)$, which is time T away from threshold. Thus the active cell can now deliver some natural number m of synaptic kicks to the other cell, thereby keeping it suppressed. The value of m can be bounded from above and below as the unique integer that satisfies

$$\frac{M - k_1(r) - k_2(r)}{k^*} - 1 < m \leq \frac{M - k_1(r) - k_2(r)}{k^*}. \quad (10)$$

Let us now show that the map $\Pi(r) = M - k_1(r) - k_2(r) - mk^*$ is decreasing on the interval $(0, g_{\min} - g_0)$. Assuming for the moment that Π is differentiable,

$$\begin{aligned}\frac{d\Pi}{dr} &= -\frac{d}{dr}(k_1(r) + k_2(r)) \\ &= -1 - \left[-e^{-\beta T(r)} + r\beta e^{-\beta T(r)}\frac{dT(r)}{dr}\right] \\ &= -[1 - e^{-\beta T(r)}] - r\beta e^{-\beta T(r)}\frac{dT(r)}{dr}.\end{aligned}$$

The first term is negative, as is the second since $dT(r)/dr > 0$. Thus $d\Pi/dr < 0$ and Π is decreasing wherever it is differentiable. To assess the continuity and differentiability of Π, note that $T(r)$ is both continuous and differentiable, which follows since the vector field of (3) is smooth between resets. Thus both $k_1(r)$ and $k_2(r)$ are differentiable. Thus the only discontinuity that can occur is when a spike is lost. More precisely if $r_1 < r_2$, it can happen that for the same value of j, $R_j(r_1) > k^*$ while $R_j(r_2) < k^*$. This would mean that there is an extra cycle of suppression associated with r_1, thereby causing a discontinuity in Π in the interval (r_1, r_2).

Now fix $r \in (g_{\min} - g_0, k^*)$. In this case, $\delta r > 0$ since the currently silent cell lies above the v-nullcline, where $v' < 0$, just after the last input of size r arrives. For the sake of argument denote this cell by c_1 and assume that the last synaptic input to this cell occurs at $t = 0$. The currently active cell, c_2, starts at $t = 0$ at the position $(0, 0)$ and after time δr will lie at $(v_2(\delta r), 0)$; see Fig. 5. Note that $v_2(\delta r)$ can be calculated directly from Eq. (1), but we only care that this value lies in $(0, 1)$. At $t = \delta r$, c_1 is reset to $v = 0$ and

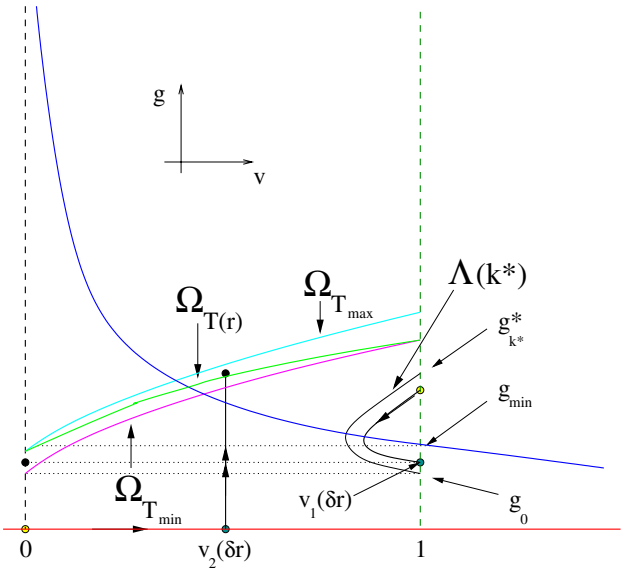

Fig. 5. The curve $\Omega_{T(r)}$ for the case $r \in (g_{\min} - g_0, k^*)$. The curve $\Omega_{T(r)}$ (green) lies between $\Omega_{T_{\max}}$ (cyan) and $\Omega_{T_{\min}}$. Yellow dots depict the initial position of cell 1 (along $v = 1$) and cell 2 (at $(0, 0)$) just after the last synaptic input. Aqua dots depict the position of the cells at time δr just before cell 1 becomes active, while the black dots represent the cell's position just after cell 1 becomes active. Note that cell 2 is reset to the curve $\Omega_{T(r)}$, which is time $T(r)$ away from threshold.

$g = (g_0 + r)\exp(-\beta\delta r) \in (g_0, g_{\min})$. Thus the time c_1 will take to reach threshold, again denoted by $T(r)$, lies between $T_{\min}$ and $T_{\max}$. In this case, unlike above, $dT(r)/dr < 0$ since the larger the r value, the smaller the value of $(g_0 + r)\exp(-\beta T(r))$ and thus the smaller the value of $T(r)$; see Fig. 4. To guarantee that c_2 becomes suppressed, c_2 must receive a synaptic kick $k_1(r)$ that causes it to be at least time $T(r)$ away from threshold. To find such a kick size we define a curve $\Omega_{T(r)}$ consisting of points that lie $T(r)$ away from threshold.

To define $\Omega_{T(r)}$, first consider two extreme cases. Observe that if $r = g_{\min} - g_0$ then $\delta r = 0$ and the time $T(r)$ is exactly $T_{\max}$. In this case, c_1 would be reset to $(0, g_{\min})$ on $\Omega_{T_{\max}}$. This will be one endpoint of $\Omega_{T(r)}$. At the other extreme, if $r = k^*$, then $\delta r = T$, c_1 is reset to $(0, g_0)$, and the time $T(r)$ is $T_{\min}$. At $t = T^-$, c_2 has evolved to $(1^-, 0)$ and is reset to the curve $\Omega_{T_{\min}}$ at $v = 1^-$ with $g > g^*_{k^*}$. This reset point will be the other endpoint of $\Omega_{T(r)}$. In general, for any $r \in (g_{\min} - g_0, k^*)$, c_2 evolves along the $(g = 0)$-axis to a point $v_2(\delta r) \in (0, 1)$ until c_2 is reset to a point located a time $T(r)$ away from threshold. By the intermediate value theorem and the monotonicity of $T(r)$ on this interval,

for each r there exists a value of g and a corresponding point in phase space lying between $\Omega_{T_{\min}}$ and $\Omega_{T_{\max}}$ that is exactly $T(r)$ away from threshold. For $r \in (g_{\min} - g_0, k^*)$,we define $\Omega_{T(r)}$ as a curve containing all such points. Note that $\Omega_{T(r)}$ is a monotone increasing curve that has endpoints at $v = 0$ on $\Omega_{T_{\max}}$ and at $v = 1$ on $\Omega_{T_{\min}}$. We set $k_1(r)$ as the g-coordinate of $(\Omega_{T(r)})^+$. It is clear by inspection that $dk_1(r)/dr > 0$. Note that c_2 ends up at $(1^-, k_1(r)\exp(-\beta T(r)))$ at $t = T(r)$. Thus, similarly to the first case, we set $k_2(r) = g^*_{k^*} - k_1(r)\exp(-\beta T(r))$, and subsequent kicks have size $k_j = k^*$.

We now show that $\Pi(r)$ is piecewise decreasing on $(g_{\min} - g_0, k^*)$ under the assumptions of the theorem. As before, a discontinuity can arise when a spike is lost if $\Pi(r) = 0$. Away from all discontinuities, calculate $d\Pi/dr$ to find

$$\frac{d\Pi}{dr} = -\frac{dk_1}{dr}[1 - e^{-\beta T(r)}] - k_1\beta\frac{dT}{dr}e^{-\beta T(r)}. \quad (11)$$

The first term is negative, but the second is positive since $dT(r)/dr < 0$ in this case. If dT/dr is sufficiently small, then $\Pi'(r) < 0$. Otherwise, note that as β grows, dT/dr goes to 0. Indeed, for each $r \in (g_{\min} - g_0, k^*)$, $T(r)$ is the time of evolution from a point $(v, g) \in \{v = 0, g \in (g_0, g_{\min})\}$ to the set $\{v = 1\}$. The largest such time is $T(g_{\min} - g_0) \equiv T_{\max}$, achieved for $g = g_{\min}$, while all of these times are bounded below by T. Both $g_{\min}$ and T are independent of β and $T(g_{\min} - g_0) \to T$ as $\beta \to \infty$, such that the whole $T(r)$ curve collapses to T. Thus, if dk_1/dr stays bounded away from 0 as β grows, then for β sufficiently large, $\Pi'(r) < 0$ on $(g_{\min} - g_0, k^*)$ (also see the remark following the proof).

Next, consider points of discontinuity of $\Pi(r)$. These occur where $\Pi(r)$ tends to 0 from above as r increases and a spike is lost. For r above this point, the input that no longer goes to the extra spike is left over for the final remainder kick of size r, which can be at most k^*. That is, in the limit as r decreases to a discontinuity, $\Pi(r) \uparrow k^*$, and thus $\Pi(r)$ jumps from 0 to k^* at each discontinuity.

Finally, we show that $\Pi(r)$ must have a fixed point. If $\Pi(0) = 0$, then we are done. Thus assume that $\Pi(0) \neq 0$. If there exists $\hat{r}$ such that $\Pi(\hat{r}) = 0$, then since the map is decreasing and continuous on $(0, \hat{r})$, it must have a fixed point on this subinterval. If no such $\hat{r}$ exists, then the map is decreasing and continuous on the entire interval $(0, k^*)$ and must cross the identity line creating a fixed point. Note that when the map has a discontinuity at $r = \hat{r}$, there must exist another fixed point to the right of $\hat{r}$. Indeed each discontinuity of the map forces the existence of another fixed point to the right of the discontinuity. By construction, the fixed point corresponds to a synaptically exhaustive, optimally periodic solution of (3), (2), as claimed. ■

Remark 3.2

(1) Numerical simulations, discussed in detail in the next subsection, show that $\Pi(r)$ is always decreasing. Furthermore, as β is increased with all other parameters fixed, the slope of $\Pi(r)$ stays rather constant except for r just above $g_{\min} - g_0$, where it becomes more negative as β increases. The larger negative slopes suggest that an unstable fixed point may occur for β sufficiently large, leading to interesting dynamics that could be studied in the future but are beyond the scope of this work.

(2) The assumption that dk_1/dr stays bounded away from 0 as β increases is quite natural. Indeed, we can show that the function $k_1(r)$ grows arbitrarily large as β increases. As β increases, $g_0 \downarrow 0$ and $g^*_{k^*} \to \infty$ so the relevant interval of r values tends to $(g_{\min}, \infty)$. At the lower limit, $k_1(g_{\min})$ remains equal to $g_{\min}$, as discussed in the proof of Theorem 1, for all β. On the other hand, no matter how large β is, as r approaches k^* from below, the active cell evolves to $(v, g) = (1^-, 0)$ in time δr. Furthermore, the point on $\Omega_{T(r)}$ corresponding to this limit in r, namely the right endpoint of $\Omega_{T(r)}$, exceeds $g^*_{k^*}$, since it takes fixed time T to pass from $(v, g) = (1^-, g^*_{k^*})$ to $(v, g) = (1^-, g_0)$ for all β and $T(r) > T$ (e.g. see Fig. 3). Thus, the difference in k_1 values at the endpoints of the relevant interval of r, which can be computed for fixed β, grows at least as fast as the length of the interval as β increases. What we do not know rigorously at this point is whether dk_1/dr stays bounded away from 0 locally in r.

3.3. *Numerical computation of* $\Pi(r)$

To illustrate the validity of the construction of $\Pi(r)$ and our results regarding its properties, we computed examples of $\Pi(r)$ numerically, as shown in Fig. 6. For $r > g_{\min} - g_0$, completing this computation using forward integration of multiple initial value problems would be somewhat problematic. That is, for a given initial value of r, we would

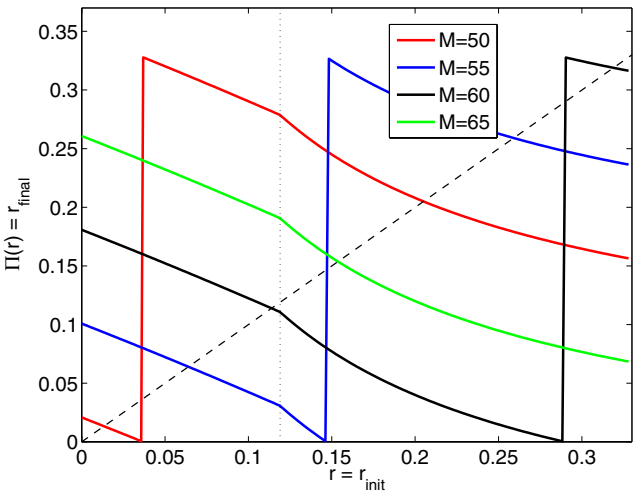

Fig. 6. Numerical examples of $\Pi(r)$ for $\beta = 0.5$, $E = -0.1$, $I = 2$ and various values of M. The dashed black line is the identity line and the dotted black line marks $r = g_{\min} - g_0$. Note that depending on parameters there may be more than one fixed point of the map.

need to flow the trajectory from the initial condition $(v_1, g_1) = (1^-, g_0 + r)$ forward to find the time $\delta r > 0$ such that $v_1(\delta r) = 1$, taking cell 1 as the initially suppressed cell and cell 2 as the initially active cell for concreteness. Next, we would need to flow the trajectory from $(v_2, g_2) = (0, 0)$ forward for time δr to obtain a value $v_2(\delta r)$. Third, we would need to flow cell 1 forward from its reset value at $(v_1, g_1) = (0, g_1(\delta r) := (g_0 + r)e^{-\beta \delta r})$ until a time $T(r) > 0$ such that $v_1(T(r)) = 1$. Finally, we would need to flow $(v_2, g_2) = (v_2(\delta r), k_1(r))$ forward for time $T(r)$ as well. The complication in this step is that the value of $k_1(r)$, selected such that $v_2(T(r)) = 1$, is not analytically accessible.

To circumvent this difficulty and make the computations more efficient, we computed $\Pi(r)$ by solving a double boundary value problem in XPPAUT. This approach allows us to find the unknowns

$$\{\delta r, g_1(\delta r), v_2(\delta r), T(r), k_1(r)\} \tag{12}$$

simultaneously, with one run of a boundary value solver. There are three important steps required to make this approach work. The first is to introduce four different pairs of (v, g) variables, one corresponding to each of the initial value problems described above. We refer to these as $(v, g), (\hat{v}, \hat{g}), (\tilde{v}, \tilde{g})$, and (v^*, g^*) in the equations below, with the exception that $\hat{g}$ does not appear since $\hat{g} \equiv 0$, corresponding to the evolution of cell 2 for time δr while cell 1 is still suppressed. The second step is to define two different time scale parameters, which we call P and Q. The parameter P is used as a time constant in the ODEs for the variables evolving for time δr, namely $(v, g), (\hat{v}, \hat{g})$, and the parameter Q appears as a time constant in the ODEs for the variables evolving for time $T(r)$, namely $(\tilde{v}, \tilde{g}), (v^*, g^*)$. Taking this step allows us to collapse all of our equations and conditions into a single boundary value problem to be solved over a fixed time interval $t \in [0, 1]$, with boundary conditions at $t = 0$ and $t = 1$. The third step is to define the boundary conditions and equations appropriately. It turns out that there are nine conditions to satisfy, and thus we need nine ODEs in our system. The equations for the evolving copies of v and g only constitute seven of these, since $\hat{g} \equiv 0$ does not appear. Because we wish to solve for P and Q, to obtain the values of δr and $T(r)$ respectively, we introduce the trivial equations $P' = 0$ and $Q' = 0$ as our eighth and ninth ODEs.

Altogether, our boundary value problem reads

$$\begin{aligned}
v' &= P(I - v - g(v - E)),\\
g' &= P(-\beta g),\\
\tilde{v}' &= Q(I - \tilde{v} - \tilde{g}(\tilde{v} - E)),\\
\tilde{g}' &= Q(-\beta \tilde{g}),\\
\hat{v}' &= P(I - \hat{v}),\\
(v^*)' &= Q(I - v^* - g^*(v^* - E)),\\
(g^*)' &= Q(-\beta g^*),\\
P' &= 0, \quad Q' = 0,
\end{aligned} \tag{13}$$

where

$$\begin{aligned}
v(0) &= 1, \quad v(1) = 1,\\
g(0) &= g_0 + r,\\
\hat{v}(0) &= 0,\\
\tilde{v}(0) &= 0, \quad \tilde{v}(1) = 1,\\
\tilde{g}(0) &= g(1),\\
v^*(0) &= \hat{v}(1), \quad v^*(1) = 1.
\end{aligned} \tag{14}$$

For fixed $\beta > 0$ and $E < 0 < I$, we can calculate $g_{\min}$ and numerically obtain $g_0, g^*_{k^*}$. With these in hand, solving the boundary value problem (13), (14) over a mesh of values $r \in (g_{\min} - g_0, k^* \equiv g^*_{k^*} - g_0]$ gives us all of the unknowns listed in (12) for each r as well as $g^*(T(r))$. From this last value, we

compute $k_2(r) = g^*_{k^*} - g^*(T(r))$. Finally, $\Pi(r)$ is obtained as

$$\Pi(r) = M - k_1(r) - k_2(r) - \left\lfloor \frac{M - k_1(r) - k_2(r)}{g^*_{k^*} - g_0} \right\rfloor (g^*_{k^*} - g_0), \quad (15)$$

where $\lfloor \cdot \rfloor$ denotes the integer floor function, where the final product in (15) is mk^* in our earlier notation, and where the same M, chosen to exceed $k_1(r) + k_2(r)$ for all r under consideration, is used for all r. For $r \in (0, g_{\min} - g_0)$, $k_1(r) = g_0 + r$ and direct forward integration from $(v, g) = (0, g_0 + r)$ for time $T(r)$ such that $v(T(r)) = 1$ gives $k_2(r) = g^*_{k^*} - g(T(r))$, such that Eq. (15) can again be employed to compute $\Pi(r)$.

Examples of the resulting $\Pi(r)$ for several M values and $\beta = 0.5,\ E = -0.1,\ I = 2$ are shown in Fig. 6. Other parameter choices gave qualitatively similar results (data not shown). There are several features to notice in Fig. 6. First, note that $g_{\min} - g_0 \approx 0.121$, as indicated with a dotted vertical line. $\Pi(r)$ is decreasing on both sides of this line, and across this line as well, except where it jumps vertically for $M = 50, 55, 60$. The jumps in these cases occur because the integer value of the floor function drops by one as r increases, corresponding to a unit decrease of m and the loss of spike. Once one fewer spikes is fired, one fewer kick of size $g^*_{k^*} - g_0$ is needed and hence the final value of r becomes relatively much larger. Another feature to note is that for all choices of M, there exists at least one and possibly more fixed points of the map. As stated in the proof of Theorem 1, the map must have a fixed point because of the fact that it is piecewise decreasing and the only discontinuity that can occur happens when $\Pi(r) = 0$. Based on the graph of these curves in Fig. 6, these fixed points all appear to be stable, but this stability is not always maintained; for example, an unstable fixed point arises when $\beta = 5.0,\ M = 50$ (data not shown). We will return to this topic in the discussion.

As M increases with other parameters fixed, progressively more spikes are fired in each cycle. In the example in Fig. 6, for $M \in \{50, 55, 60, 65\}$, the numbers of spikes are $\{(149, 148), (164, 163), (179, 178), (194)\}$, where the pairs provide spike numbers before and after points of discontinuity. The linear scaling of spikes with M makes sense, since $k_1(r), k_2(r), g^*_{k^*}$, and g_0 are independent of M. Furthermore, we note in Fig. 6 that as M is varied, the slopes along the corresponding segments of the graph remain the same. This relation is also consistent with (15), which shows that the slope of these graphs in between spike subtractions is independent of M.

The observation that $\Pi(r)$ always has a fixed point for fixed M leads us naturally to the question of what happens when M is no longer fixed, but rather is determined by the rate of the recovery of synaptic resources that occurs while a cell is suppressed. We turn to this question in the next subsection.

3.4. *Recovery of synaptic resources*

The argument in Sec. 3.2 shows that a certain synaptic release pattern yields a synaptically exhaustive, optimally periodic, anti-phase bursting solution for any fixed M sufficiently large, assuming full recovery of synaptic resources back to the level M between active spiking phases for each cell. Now, let us more carefully consider the issue of recovery of synaptic resources while a cell is suppressed. Denote available resources as R and assume that while a cell is suppressed

$$R' = \rho(S - R), \quad (16)$$

where $\rho > 0$ is a synaptic recovery rate and $S > M > 0$ is a maximal level of resources available to each cell. To be consistent with our earlier analysis, assume that $R(0) = 0$ for a formerly active cell when it first becomes suppressed and ignore recovery between spikes within an active phase. To achieve recovery to the level $R = M$ under Eq. (16) with $R(0) = 0$ requires time

$$t^* = -\frac{1}{\rho} \ln\left(1 - \frac{M}{S}\right).$$

For consistency, we require $t^* = \tau/2$, where τ is the period of the full bursting solution (including active phases for both cells). This condition yields

$$T(r) + (m+1)T + \delta r = -\frac{2}{\rho} \ln\left(1 - \frac{M}{S}\right), \quad (17)$$

where $T(r)$ is the time it takes for the first spike in the burst to be fired, which by construction differs from T.

There are many ways to guarantee that (17) holds. For example, the left-hand side of Eq. (17) increases linearly in M, since m does. But the right-hand side has a vertical asymptote at $M = S$ and

hence exceeds the left-hand side for $S - M > 0$ sufficiently small. Based on their slopes and the intermediate value theorem, the two sides agree at a unique value of $M \in (2\hat{g}, S)$ provided that the left-hand side of (17) exceeds that right-hand side at $2\hat{g}$. The most straightforward condition that ensures that this result holds is if S is sufficiently large, as the existence of the anti-phase bursting solution simply requires sufficiently large M and is not affected by still larger choices of S, while increasing S can make the right-hand side of (17) become arbitrarily small for each fixed M. Thus, we have shown:

Theorem 2. *Fix $\overline{M} > 0$ such that Theorem 1 holds. For S sufficiently large, there exists a value $M > \overline{M}$ such that a synaptically exhaustive, optimally periodic anti-phase bursting solution exists in which the synaptic resources of each cell are fully exhausted during each active phase and recover under Eq. (16) to the level M during each silent phase.*

Another way that (17) can hold is to fix $M > 0$ such that Theorem 1 holds. Then the left-hand side of (17) is a constant. The right-hand side has the two free parameters S and ρ. If we fix $S > M$, then clearly as $\rho \to 0$, the right-hand side increases monotonically and is unbounded. Thus there exists a unique value of ρ at which (17) holds. This leads to a second formulation of the existence of the anti-phase bursting solution.

Theorem 3. *Fix $M > 0$ such that Theorem 1 holds. For each $S > M$, there exists a value of ρ such that a synaptically exhaustive, optimally periodic anti-phase bursting solution exists in which the synaptic resources of each cell are fully exhausted during each active phase and recover under Eq. (16) to the level M during each silent phase.*

Remark 3.3. We could generalize the above analysis to include recovery of synaptic resources in between spikes during each active phase. The expressions involved would become more complicated, however, without any new insights being gained. The above analysis can be thought of as the specialization of the more general case to the regime in which interspike intervals are quite short relative to interburst intervals, which is exactly the typical scenario for neuronal bursting.

3.5. *Dynamics of the map $\Pi(r)$ and optimal strategies for anti-phase bursting*

As noted earlier, $\Pi(r)$ is a piecewise decreasing map of the interval $[0, k^*)$ into itself. Because discontinuities can only occur at values where $\Pi(r^-) = 0$ and $\Pi(r^+) = k^*$, the map must have a fixed point for any fixed M above some value. Theorems 2 and 3 imply the existence of a synaptically exhaustive, optimally periodic solution with recovery of synaptic resources, corresponding to the fixed point r^* of $\Pi(r)$ for some specific choice of M. The period of this solution is $2(T(r) + T + mT + \delta r)$ where $\delta r = 0$ if $r^* \in (0, g_{\min} - g_0)$ and $\delta r > 0$ if $r^* \in (g_{\min} - g_0, k^*)$. We express the period in this manner to show explicitly how the various interspike intervals contribute. Namely, $T(r) + T$ represent the interspike intervals caused by synaptic kicks $k_1(r)$ and $k_2(r)$, mT are the m interspike intervals associated with subsequent kicks, and δr is associated with the final synaptic kick.

We have not considered the stability of the fixed point since its stability does not imply stability of the optimally periodic solution. Indeed, the stability of r^* would only yield information about how the coupled system responds to perturbations in the last kick size but not, for example, perturbations in the spike times of the active cell or synaptic kick sizes prior to the last one. Given stability of the fixed point, however, we can exploit perturbations in kick sizes to determine alternative optimal synaptic strategies. That is, we consider an optimal strategy that a cell can use to be one that maximizes the number of spikes it can fire in a burst. Given this definition, there may not be a unique optimal strategy. Rather, there could be an infinite collection of strategies that will allow each cell to fire $m+3$ spikes per burst. We describe these here. All strategies are variations of some sort on the solution that we found above in Theorems 2 and 3, although the actual anti-phase burst solution may technically not be a periodic orbit of the dynamical system governed by Eqs. (2)–(4) and hence we refer to such solutions as optimal but not optimally periodic.

Theorem 4. *If $\Pi(r)$ has a globally stable fixed point r^* with $m \geq 3$, then there exist infinitely many synaptic strategies that lead to a synaptically exhaustive, optimal anti-phase bursting solution. More precisely, assume that M, S and ρ are chosen such that Theorem 2 or Theorem 3 holds,*

with an associated synaptic strategy given by kicks $\{k_i^*\}$ *for* $i = 1, \ldots, m+3$ *yielding a globally stable fixed point* r^* *of* Π. *Then there exists an infinite set of synaptic strategies* $\{k_i\}$, $i = 1, \ldots, m+3$ *such that each leads to a synaptically exhaustive, optimal anti-phase bursting solution. For each of these strategies, for each* $i \in \{1, \ldots, m\}$, $k_i = k_i^* + \epsilon_i$ *with* $\epsilon_i \in [0, r^*]$, *and for each strategy,*

$$\sum_{i=1}^{m+3} \epsilon_i = r^*. \tag{18}$$

Proof. For fixed M, suppose that Π has a globally stable fixed point given by $r^* \in (0, k^*)$ corresponding to a synaptically exhaustive, optimally periodic anti-phase bursting solution with $m+3$ spikes per active phase. For this solution, the residual synaptic resources left for the final spike in each active phase are not sufficient to suppress the silent cell for one more cycle. Thus, they are largely meaningless in maximizing the number of spikes the active cell can fire. Hence by redistributing some or all of r^* among the $m+2$ spikes before the final one, we will not change the number of spikes that occur within a burst.

Suppose that for the first $m-1$ kicks, $k_i = k_i^*$. Now, suppose that upon the mth spike, the active cell gives the silent cell a kick of size $k_m = k_m^* + \epsilon_m$ with $\epsilon_m \in (0, r^*)$. When the $(m+1)$st spike is fired, the silent cell has $g = g_0 + \epsilon_m e^{-\beta T}$. Suppose that the kick on this spike is of size $k_{m+1} = k_{m+1}^* + \epsilon_{m+1}$ with $\epsilon_{m+1} < 0$ selected to place the trajectory of the silent cell on Ω_T, say with $g = g_{m+1} < g_{k^*}^*$. When the $(m+2)$nd spike is fired, the silent cell has $v = 1^-$ and $g = g_{m+1} e^{-\beta T}$. Choose $k_{m+2} = k_{m+2}^* + \epsilon_{m+2} = g_{k^*}^* - g_{m+1} e^{-\beta T}$, to place the trajectory at $(1^-, g_{k^*}^*)$, from which it will evolve to $(1^-, g_0)$ in time T. Note that $k_{m+2}^* = g_{k^*}^* - g_0$ and because trajectories from Ω_T cannot cross $\Lambda(k^*)$, $g_{m+1} e^{-\beta T} < g_0$, such that $\epsilon_{m+2} > 0$. Finally, let $k_{m+3} = k_{m+3}^* + \epsilon_{m+3}$ with ϵ_{m+3} chosen to satisfy (18).

There are two conditions we must check to ensure that the above choices are feasible. One is that synaptic resources available at the $(m+2)$nd spike are at least equal to $g_{k^*}^* - g_{m+1} e^{-\beta T}$. Mathematically, this condition takes the form

$$r^* + k_{m+2}^* - \epsilon_{m+1} - \epsilon_m \geq g_{k^*}^* - g_{m+1} e^{-\beta T},$$

or, since $k_{m+2}^* = g_{k^*}^* - g_0$,

$$r^* - \epsilon_{m+1} - \epsilon_m \geq g_0 - g_{m+1} e^{-\beta T}. \tag{19}$$

As $\epsilon_m \to 0$, it is clear that $\epsilon_{m+1} \to 0$. In addition, $g_{m+1} \to g_{k^*}^*$, and by definition, $g_0 = g_{k^*}^* \exp^{-\beta T}$. Thus the right-hand side also tends to 0. The positive term r^* is independent of ϵ_m, so we can ensure that condition (19) holds for ϵ_m sufficiently small. Secondly, we need the synaptic resources remaining at the $(m+3)$rd spike to be small enough that the final kick keeps $g < g_{k^*}^*$. Mathematically, this condition is

$$g_0 + k_{m+3}^* + \epsilon_{m+3} < g_{k^*}^*.$$

We have $k_{m+3}^* = r^*$ and $\epsilon_{m+3} = -(\epsilon_m + \epsilon_{m+1} + \epsilon_{m+2})$. Since $g_0 + r^* < g_{k^*}^*$, this condition also holds for ϵ_m sufficiently small.

These choices of perturbations ensure that the silent cell remains suppressed in a way that allows the active cell to fire $m+3$ spikes. For ϵ_m sufficiently small, the silent cell trajectory has $g = g_{m+3} \in (g_0, g_{k^*}^*)$ after it receives input k_{m+3}. Moreover, at that time, it has $v = 1^-$. Hence, the silent cell spikes before the active cell can spike again. The stability of r^* ensures that following the original strategy on subsequent cycles will yield convergence of the synaptic remainder back towards r^*. Once the trajectory is sufficiently close to the optimally periodic solution, an alternative strategy as described above can be selected again without loss of optimality.

The above argument already supplies infinitely many optimal strategies, since ϵ_m can be any sufficiently small positive real number. Furthermore, the same idea can be applied to spikes before spike m, specifically to spikes $3, \ldots, m$, as long as the perturbed kicks are sufficiently small that (18) can be satisfied in a way that yields $g_{m+3} \in (g_0, g_{k^*}^*)$. ■

In practice, the fact that $\Lambda(k^*)$ is attracting suggests that the special choices of $\epsilon_{m+1}, \epsilon_{m+2}$ would not be needed to attain optimality, at least for m sufficiently large. Similarly, we expect that sufficiently small perturbations to all k_i^* would maintain optimality without these adjustments, and that local stability of r^* would suffice to allow optimality to persist under these small perturbations.

In the event that there are two fixed points $r_1^* < r_2^*$ of Π, the smaller valued fixed point corresponds to a burst with $m+3$ spikes versus $m+2$ for the larger one. The optimal strategy is therefore the one associated with r_1^*. If the network is operating with the strategy associated with r_2^*, then at the start of the next burst, it should reallocate k_1

and k_2 to redirect the solution towards the fixed point r_1^*.

Solutions found in this way suggest that the optimal strategy is robust and to some degree insensitive to the exact value of the synaptic input. In other words, small changes in synaptic kick sizes are permissible so long as each kick (except for the last) remains above k^*. In this sense, the class of optimal strategies is also robust to noise and perturbations, with the degree of robustness corresponding to the size of the residual synaptic resources, r^*, left over at the final spike of each burst.

3.6. *1-1 anti-phase solutions*

For this section, we present a proof of 1-1 anti-phase spiking since the above analysis applies only to the bursting case. We again neglect recovery of synapses between spikes and we consider solutions in which the two cells take turns firing, with equal interspike intervals. Mathematically, if we let 2τ denote the period of these solutions and $v_1(t^-) = 1$ with $g_1(t^-) = k$ for some t, then we have $(1, k) = (v_1(t + 2\tau), g_1(t + 2\tau)) = (v_1(t + 4\tau), g_1(t + 4\tau)) = \cdots = (v_2(t + \tau), g_2(t + \tau)) = (v_2(t + 3\tau), g_2(t + 3\tau)) = \cdots$ and $(v_2(t), g_2(t)) = (v_2(t + 2\tau), g_2(t + 2\tau)) = \cdots = (v_1(t + \tau), g_1(t + \tau)) = (v_1(t + 3\tau), g_1(t + 3\tau)) = \cdots$; that is, the two cells exchange positions from one firing event to the next.

First, consider a segment $\{(v, g) : v = 1, 0 \leq g \leq g_{\min}\}$ at threshold. Suppose we flow this segment backwards in time under the time-reversed flow of (3). Obviously, the trajectory emanating from its bottom endpoint simply lies along $\{g = 0\}$. On the other hand, the trajectory emanating from a point $(1, g)$ for g sufficiently close to $g_{\min}$ intersects the v-nullcline at some minimal value of v and then continues back towards $\{v = 1\}$. By shooting, there exists a $g^- \in (0, g_{\min})$ such that under the backwards flow of (3), $(1, g^-) \cdot t \to (E, \infty)$ as $t \to \infty$ (here, t refers to backwards time).

For each $g \in [0, g_{\min}]$, compare the forward trajectory of (3) from $(0, g)$, which belongs to the set $\{0 \leq v \leq 1\}$, say $\gamma_0^+(g) = \{(v, g) = (v_0^+(t; g), ge^{-\beta t}) : t \geq 0, v \leq 1\}$, to the backward trajectory from $(1, g)$ inside $\{0 \leq v \leq 1\}$, say $\gamma_1^-(g) = \{(v, g) = (v_1^-(t; g), ge^{\beta t}) : t \geq 0, v \leq 1\}$ (where in the latter case we again abuse notation and use t to refer to backwards time). For each $g \in [0, g^-]$, there exists a unique $t(g)$ such that $v_0^+(t(g); g) = v_1^-(t(g); g) \in (0, 1)$; for $g = 0$, for example, $t(0) = T/2$. By continuity, such $t(g)$ also exists for $g > g^-$ as long as $g - g^-$ is sufficiently small. On the other hand, for $g = g_{\min}$, the backwards flow immediately leaves $\{v \leq 1\}$ as soon as $t > 0$, so $t(g_{\min})$ is not defined. Let $\tilde{g} = \sup\{g \in [0, g_{\min}] : t(g) \text{ exists on } [0, g]\} > g^-$.

Proposition 3. *For each $g \in [0, \tilde{g}]$, there is a synaptic kick size*

$$\tilde{k}(g) = g(e^{\beta t(g)} - e^{-\beta t(g)}) > 0 \tag{20}$$

for which there exists a periodic 1-1 solution with reset conditions $(v, g) \mapsto (0, g)$ for the firing cell and $(v, g) \mapsto (v, g + \tilde{k}(g))$ for the nonfiring cell. The period of the solution is $2t(g)$.

Proof. Fix $g \in [0, \tilde{g}]$ and let $\tilde{k}(g)$ be defined by Eq. (20). Choose the initial condition $(v_1, g_1)(0) = (0, g)$ for cell 1 and the initial condition $(v_2, g_2)(0) = (v_1^-(t(g); g), ge^{\beta t(g)})$ for cell 2. The choice of initial conditions for cell 2 ensures that after time $t(g)$, $v_2(t(g)^-) = 1$ and $g_2(t(g)^-) = g$. Thus, cell 2 fires at time $t(g)$ and is reset to $(v_2(t(g)^+), g_2(t(g)^+)) = (0, g)$, which is exactly the initial position of cell 1. The definition of $t(g)$ implies that after time $t(g)$, $v_1(t(g)^-) = v_2(0)$, while $g_1(t(g)^-) = ge^{-\beta t(g)}$. Because cell 2 fires, $g_1(t(g)^+) = g_1(t(g)^-) + \tilde{k}(g) = g_2(0)$, while $v_1(t(g)^+) = v_2(0)$. Thus, after time $t(g)$, cell 1 has assumed the initial position of cell 2. In summary, after the reset, the two cells have switched places, and a 1-1 anti-phase solution results. ■

Note that the synaptic kick size $\tilde{k}(g)$ from Eq. (20) is a strictly increasing function of g, with $\tilde{k}(0) = 0$. Thus, the set of kick sizes for which 1-1 solutions exist is bounded above by $\tilde{k}(\tilde{g})$. Larger resets will result in solutions for which one cell remains suppressed for more than 1 spike of the other cell, at least on some cycles.

4. Discussion

The primary focus of this paper has been the derivation and analysis of the one-dimensional map $\Pi(r)$. Maps that are derived in the context of coupled neuronal networks often are either Poincaré maps in the phase space of the dynamic variables or interspike interval maps that strobe the network each time a spike occurs. Our map $\Pi(r)$ is instead a generalized return map, defined at a particular spiking event, but one that is based on a quantity r that is not an explicit variable of the model under study but

rather a derived quantity that turns out to be useful. The map-based approach used here is somewhat similar in style to earlier analysis of the induction of activity using an event-based map [Rubin & Bose, 2006], but the details are quite different. We developed a novel method to numerically solve a double boundary value problem to be able to compute the graph of the map. We were analytically able to explain many of the properties observed in our numerical results. We find fixed points of $\Pi(r)$ that correspond to anti-phase solutions in which each unit in our two-cell network fires a burst of maximal length, meaning that it fires as many spikes as possible, or equivalently stays active for the longest possible time, before the other unit activates and takes over.

Somewhat unexpectedly, the map $\Pi(r)$ exhibits coexistence, and apparent bistability, of fixed points for a wide range of parameter sets. This is a consequence of two facts: one, $\Pi(r)$ is piecewise decreasing, and two, the nature of the discontinuity forces the jump at the discontinuity to be an increase across the entire range of the map. Piecewise continuous maps often give rise to quite complicated dynamics and even chaos through border collision bifurcations [Nusse & Yorke, 1992]. For the range of β values that we focused on, although the discontinuity of $\Pi(r)$ moves, the fixed points of the map continue to exist and do not lose stability, such that complicated dynamics are avoided. We do note, however, that as β increases, our exploratory numerical results suggest that the slope of the map may drop below -1. This effect only arises near the transitional point $r = g_{\min} - g_0$, but it may induce unstable fixed points (e.g. for $\beta = 5.0,\ M = 50$). In turn, this instability raises the possibility of more interesting dynamics that remain to be further explored.

After we define $\Pi(r)$, it is not difficult to enhance our model and extend our analysis to include the recovery of synaptic resources, such that the resources available to a cell when it first becomes active are determined by the evolution of a recovery equation while the cell is silent. Imposing consistency between the resources expended over the course of each spiking phase and the resources recovered during each silent phase, we find that there always exists some resource level for which the corresponding fixed point achieves consistency. That is, the constraint of dynamic resource recovery selects a particular resource level and phase duration at which the system can exhibit periodic oscillations. Furthermore, we show that, if the consistent strategy is stable as a fixed point of $\Pi(r)$, then it is in fact robust to small perturbations of the sizes of the synaptic kicks induced at each spike, which is an essential property for the use of such strategies to derive sustainable anti-phase bursting activity patterns in networks of oscillators coupled with inhibition.

The solutions that arise as fixed points of $\Pi(r)$ are optimal, in the sense that at each spike time of the active cell, the suppressed cell is itself as close as possible (in a precise mathematical sense) to the threshold. Any reduction in synaptic kick size would allow the suppressed cell to take over after fewer active cell spikes, while any small increase would correspond to wasted synaptic resources that do not lead to extra active cell spikes. On the other hand, we have not proved that these strategies achieve global maximization of spike numbers over the entire space of possible synaptic strategies. In particular, we do not compare them to "big kick" strategies [Wang *et al.*, 2011] in which one spike is accompanied by a very large release of synaptic resources that keeps the silent cell suppressed for multiple spikes of the active cell. Past work has shown that in certain parameter regimes in networks with excitatory coupling and constrained synaptic resources, big kick strategies can maximize the number of spikes that an excited neuron can fire [Wang *et al.*, 2011]. Here, we do not expect big kick strategies to be useful, because the exponential decay of the coupling variable causes it to decline by a relatively large amount within a fixed interspike interval when it begins from a large value, but we have not considered them rigorously.

This work is largely motivated by the study of central pattern generating neuronal networks that are responsible for vital motor functions. These networks often exhibit characteristic anti-phase bursting activity [Grillner, 1985; Marder & Calabrese, 1996; Marder & Bucher, 2001], and these patterns are typically produced by groups of neurons that communicate using synaptic inhibition. The period and duty cycle (ratio of burst length to period) of neurons within the oscillatory pattern are important quantities to modulate as they may lead to different motor outputs [Butera *et al.*, 1999; Marder & Bucher, 2001; Briggman & Kristan Jr., 2008]. This modulation is often achieved by specifically changing intrinsic or synaptic properties [Marder & Prinz,

2003; Mitchell & Johnson, 2003; Morris *et al.*, 2003]. In this paper, we have taken a different approach to controlling the oscillatory pattern. Namely, we have allowed the constituent elements to decide how much synaptic output is needed at each spike to achieve a desired outcome. In this case, we looked for strategies to maximize the number of spikes a neuron can fire before it uses all of its synaptic resources. Although there is currently no evidence that neuronal networks solve the optimization problem that we have posed, the robustness of the strategies we derive suggest that these could be biologically relevant and should be considered in the design and interpretation of future experiments. Our analysis also inherently reveals strategies that neurons can employ in order to fire any number of spikes up to the maximum before relinquishing control of firing to the other cell. By simply providing a synaptic kick of less than k^* after an appropriate spike, the currently active cell can initiate the switch to becoming silent. Thus, a network could be induced to switch phases prematurely by the action of a modulator that transiently compromised synaptic release, and other neuromodulatory effects on synaptic dynamics could also be considered [Hasselmo, 1995; Gil *et al.*, 1997; Marder & Bucher, 2001; Cobb & Davies, 2005; Briggman & Kristan Jr., 2008; Harris-Warrick, 2011]. We can also generalize our findings to larger networks of neurons that break up into two clusters of cells. If the network is all-to-all coupled, one can easily envision how cells from one cluster could take turns firing, individually using up their own synaptic resources, but never allowing cells from the other group to gain control of the activity pattern. Another obvious problem that can naturally be considered with this analysis is the relationship between activity patterns and synaptic strategies when a cell can provide different amounts of synaptic input to different postsynaptic targets.

There are several other extensions to our analysis that one could consider. Perhaps the most compelling and straightforward one would be to consider the effects of synaptic plasticity. If, for example, the synapses exhibited short-term synaptic depression, then the active cell would need to balance its own firing rate versus the depression and recovery rates in order to solve the optimization problem. This would add a layer of complication that would be quite interesting to model and analyze. A second natural extension would be to consider a network of neurons exhibiting activity with more than two phases. One need only consider a network of three neurons to begin exploring such questions. For example, the pyloric rhythm of the crab stomatogastric ganglion consists of three major groups of neurons firing out of phase with one another in a tri-phasic rhythm [Hooper, 1997; Mouser *et al.*, 2008]. Here a relevant question is what sets the relative phase of firing of each group of neurons. This question is directly related to how long each group remains active and what are the mechanisms responsible for the switching of cells from being silent to active. One can imagine how issues like the ones we consider may arise in establishing synaptic properties during the development of rhythmic neuronal networks.

Acknowledgments

This work was supported, in part, by grants from the National Science Foundation DMS-1122291 (AB) and DMS-1312508 (JR). J. Rubin thanks Bard Ermentrout for useful discussions about XPPAUT. The authors also thank Alex Pastena who carried out some initial simulations of this model.

References

Briggman, K. & Kristan Jr., W. [2008] "Multifunctional pattern-generating circuits," *Ann. Rev. Neurosci.* **31**, 271–294.

Butera, R., Rinzel, J. & Smith, J. [1999] "Models of respiratory rhythm generation in the pre-Bötzinger complex. II. Populations of coupled pacemaker neurons," *J. Neurophysiol.* **82**, 398–415.

Buzsaki, G. [2010] "Neural syntax: Cell assemblies, synapsembles, and readers," *Neuron* **68**, 362–385.

Chandrasekaran, L., Matveev, V. & Bose, A. [1999] "Multistability of clustered states in a globally inhibitory network," *Physica D* **238**, 253–263.

Clay, J., Forger, D. & Paydarfar, D. [2012] "Ionic mechanism underlying optimal stimuli for neuronal excitation: Role of na+ channel inactivation," *PLoS ONE* **7**, e45983.

Cobb, S. & Davies, C. [2005] "Cholinergic modulation of hippocampal cells and circuits," *J. Physiol.* **562**, 81–88.

Ermentrout, B. [1992] "Complex dynamics in winner-take-all neural nets with slow inhibition," *Neur. Netw.* **5**, 415–431.

Ermentrout, B. [2002] *Simulating, Analyzing, and Animating Dynamical Systems* (SIAM, Philadelphia).

Feng, X., Shea-Brown, E., Greenwald, B., Kosut, R. & Rabitz, H. [2007] "Optimal deep brain stimulation of the subthalamic nucleus — A computational study," *J. Comput. Neurosci.* **23**, 265–282.

Forger, D. & Paydarfar, D. [2004] "Starting, stopping, and resetting biological oscillators: In search of optimum perturbations," *J. Theor. Biol.* **230**, 521–532.

Forger, D., Paydarfar, D. & Clay, J. [2011] "Optimal stimulus shapes for neuronal excitation," *PLoS Comput. Biol.* **7**, e1002089.

Fortune, E. & Rose, G. [2001] "Short-term synaptic plasticity as a temporal filter," *Trends Neurosci.* **24**, 381–385.

Gil, Z., Connors, B. & Amitai, Y. [1997] "Differential regulation of neocortical synapses by neuromodulators and activity," *Neuron* **19**, 679–686.

Grillner, S. [1985] "Neurobiological bases of rhythmic motor acts in vertebrates," *Science* **228**, 143–149.

Harris-Warrick, R. [2011] "Neuromodulation and flexibility in central pattern generator networks," *Curr. Opin. Neurobiol.* **21**, 685–692.

Hasselmo, M. [1995] "Neuromodulation and cortical function: Modeling the physiological basis of behavior," *Behav. Brain Res.* **67**, 1–27.

Hooper, S. [1997] "Phase maintenance in the pyloric pattern of the lobster (*panulirus interruptus*) stomatogastric ganglion," *J. Comput. Neurosci.* **4**, 191–205.

Huntsman, M., Porcello, D., Homanics, G., DeLorey, T. & Huguenard, J. [1999] "Reciprocal inhibitory connections and network synchrony in the mammalian thalamus," *Science* **283**, 541–543.

Kaski, S. & Kohonen, T. [1994] "Winner-take-all networks for physiological models of competitive learning," *Neur. Netw.* **7**, 973–984.

Marder, E. & Calabrese, R. [1996] "Principles of rhythmic motor pattern generation," *Physiol. Rev.* **76**, 687–717.

Marder, E. & Bucher, D. [2001] "Central pattern generators and the control of rhythmic movements," *Curr. Biol.* **11**, R986–R996.

Marder, E. & Prinz, A. [2003] "Current compensation in neuronal homeostasis," *Neuron* **37**, 2–4.

Marder, E., Bucher, D., Schulz, D. & Taylor, A. [2005] "Invertebrate central pattern generation moves along," *Curr. Biol.* **15**, R685–R699.

Marder, E. & Bucher, D. [2007] "Understanding circuit dynamics using the stomatogastric nervous system of lobsters and crabs," *Ann. Rev. Physiol.* **69**, 291–316.

Masino, M. & Calabrese, R. [2001] "Phase relationships between segmentally organized oscillators in the leech heartbeat pattern generating network," *J. Neurophysiol.* **87**, 1572–1585.

Mitchell, G. & Johnson, S. [2003] "Invited review: Neuroplasticity in respiratory motor control," *J. Appl. Physiol.* **94**, 358–374.

Moehlis, J., Shea-Brown, E. & Rabitz, H. [2006] "Optimal inputs for phase models of spiking neurons," *ASME J. Comput. Nonlin. Dyn.* **1**, 358–367.

Morris, K., Baekey, D., Nuding, S., Dick, T., Shannon, R. & Lindsey, B. [2003] "Invited review: Neural network plasticity in respiratory control," *J. Appl. Physiol.* **94**, 1242–1252.

Mouser, C., Nadim, F. & Bose, A. [2008] "Maintaining phase of the crustacean tri-phasic rhythm," *J. Math. Biol.* **57**, 161–181.

Nabi, A., Mirzadeh, M., Gibou, F. & Moehlis, J. [2013] "Minimum energy desynchronizing control for coupled neurons," *J. Comput. Neurosci.* **34**, 259–271.

Nusse, H. & Yorke, J. [1992] "Border-collison bifurcations including "period two to period three" for piecewise smooth systems," *Physica D* **57**, 39–57.

Popovych, O. & Tass, P. [2014] "Computational model-based development of novel stimulation algorithms," *Encyclopedia of Computational Neuroscience* (Springer), pp. 1–29.

Rosenbaum, R., Rubin, J. & Doiron, B. [2012] "Short term synaptic depression imposes a frequency dependent filter on synaptic information transfer," *PLoS Comp. Biol.* **8**, e1002557.

Rosenbaum, R., Rubin, J. & Doiron, B. [2013] "Short-term synaptic depression and stochastic vesicle dynamics reduce and shape neuronal correlations," *J. Neurophysiol.* **109**, 475–484.

Rubin, J. & Terman, D. [2000] "Analysis of clustered firing patterns in synaptically coupled networks of oscillators," *J. Math. Biol.* **41**, 513–545.

Rubin, J. & Bose, A. [2006] "The geometry of neuronal recruitment," *Physica D* **221**, 37–57.

Singer, W. [1999] "Neuronal synchrony: A versatile code for the definition of relations?" *Neuron* **24**, 49–65.

Skinner, F., Kopell, N. & Marder, E. [1994] "Mechanisms for oscillation and frequency control in networks of mutually inhibitory relaxation oscillators," *J. Comput. Neurosci.* **1**, 69–87.

Smith, J., Abdala, A., Rybak, I. & Paton, J. [2009] "Structural and functional architecture of respiratory networks in the mammalian brainstem," *Philos. Trans. Roy. Soc. B: Biol. Sci.* **364**, 2577–2587.

Terman, D. & Wang, D. [1995] "Global competition and local cooperation in a network of neural oscillators," *Physica D* **81**, 148–176.

Wang, J., Costello, W. & Rubin, J. [2011] "Tailoring inputs to achieve maximal neuronal firing," *J. Math. Neurosci.* **1**, 1–32.

Zucker, R. & Regehr, W. [2002] "Short-term synaptic plasticity," *Ann. Rev. Physiol.* **64**, 355–405.

Appendix A

Here we present a general modeling framework to which the analysis done in this paper will generalize, such that we can identify strategies that give rise to optimal anti-phase bursting solutions. Consider a pair of oscillators coupled through mutually inhibitory interactions, defined more precisely below. Assume that a certain variable quantifies the state of each oscillator and that when this variable reaches a threshold, an oscillator is able to (i) fire a spike, and (ii) determine the strength with which it inhibits the other oscillator. Suppose we impose a reset condition such that once an oscillator's state variable reaches threshold, it drops back to some low level. Finally, assume that each time an oscillator fires, the amount by which it boosts its inhibition of the other oscillator is independent of the boosts associated with all other firing events. Within the inhibitory two-oscillator network, we refer to the unit that most recently reached threshold as *active* and the other as *silent*.

Suppose that at some time t_0, a silent oscillator activates and thus switches to active and renders the other oscillator silent. Suppose that the newly active oscillator stays active until a switching time $t_s > t_0$. Without loss of generality, let $t_0 = 0$. Mathematically, we write the equations that govern the behavior of a silent oscillator for $t \in [0^+, t_s]$ as

$$\begin{aligned} x' &= f(x, g), \\ g' &= -\beta g + \sum_i k_i \delta(t - t_i) \end{aligned} \tag{A.1}$$

where f is smooth in both arguments and $\{t_i\}, i = 1, \ldots, N$ is a finite collection of times with $t_{i-1} < t_i$ for $i \geq 2$ and each $t_i \in (0, t_s)$. The times $\{t_i\}$ correspond to spike times of the active oscillator. We assume that $\sum_i k_i \leq M$, where $M > 0$ is some bound and the sum is over the N inhibitory boosts that the oscillator receives during all the consecutive activations of the active oscillator; for now we leave N unspecified. We also assume that:

(A0) $f(0, g) > 0$ for all g,
(A1) $\partial f/\partial g < 0$, such that g corresponds to an inhibitory input,
(A2) $\partial f/\partial x < 0$, and
(A3) $f(x, g) = 0$ has a solution $g = g(x)$ such that $g(x^*) = 0$ for some $0 < \theta < x^* < \infty$, with θ defined below. Note that differentiation of $f(x, g(x)) = 0$ yields $g'(x) < 0$, by (A.1) and (A.2).

We fix equations for the active oscillator for $t \in [0^+, t_s]$ based on a threshold $\theta > 0$ as

$$\begin{aligned} y' &= \begin{cases} f(y, h), & 0 < t < t_1 \\ f(y, 0), & t_1 < t \leq t_s \end{cases} \\ h' &= -\beta h, \quad 0 < t < t_1, \end{aligned} \tag{A.2}$$

where $t_1 = \inf\{t > 0 : y(t) = \theta\}$, which we assume is a well-defined positive number, and we no longer track h after time t_1. We also assume that the synaptic resources of the silent cell follow the synaptic recovery equation (4) and we impose the reset condition $y(t) = \theta \Rightarrow y(t^+) = 0$, such that $y(t_i) = \theta$ for all $i = 1, \ldots, N$. With this notation, our definition of t_s means that $0 \leq x < \theta$ for all $t \in (0, t_s)$, that $t_1 < t_s$, and that $x(t_s) = \theta$, $y(t_s) < \theta$ both hold. Our use of $y' = f(y, 0)$ for $t \in (t_1, t_s)$ is an approximation motivated by the idea that when the inhibition to an oscillator gets sufficiently small, its effect is negligible.

Consider a pair of oscillators described by variables (u, v, a, b, P, Q) defined as follows: u, v represent the states of the oscillators, a is the strength of the inhibition from the v-oscillator to the u-oscillator, b is the strength of the inhibition from the u-oscillator to the v-oscillator, P is the amount of resources that v has available to inhibit u, and Q is the amount of resources that u has available to inhibit v. We can define one cycle of a periodic oscillation of period $\tau_P + \tau_Q$ as a function (u, v, a, b, P, Q) of time such that (u, a) satisfy system (A.1) for $t \in (0, \tau_P)$ and system (A.2) for $t \in (\tau_P, \tau_P + \tau_Q)$, while (v, b) satisfy the same systems on complementary time intervals, with $u(\tau_P) = \theta, v(\tau_P) < \theta$, $v(\tau_P + \tau_Q) = \theta, u(\tau_P + \tau_Q) < \theta$, such that switching occurs at times τ_P and $\tau_P + \tau_Q$, and also such that P satisfies Eq. (4) on $(0, \tau_P)$ and Q satisfies Eq. (4) on $(\tau_P, \tau_P + \tau_Q)$.

We choose initial conditions to ensure continuity and extend this to a periodic oscillation on all time in the natural way. Specifically, for the sake of simplicity, let $\tau/2 = \tau_P = \tau_Q$. Then for a periodic oscillation to be well-defined, there must exist a natural number N, a sequence of times $\{t_i\}$, $i = 1, \ldots, N$ in $(0, \tau/2)$ as described above, and a sequence of kicks $\{k_i > 0\}$, $i = 1, \ldots, N$ together with an $M \geq \sum_i k_i$ such that if $P(0) = s_0 := M - \sum_i k_i$ and P flows under Eq. (4), then $P(\tau/2) = M$. We impose this s_0 as our value

for $P(0)$ and for $Q(\tau/2)$ and assume that P and Q are governed by (4) on $(0, \tau/2)$ and $(\tau/2, \tau)$, respectively, such that $P(\tau/2)$=M and $Q(\tau) = M$. To form a periodic orbit, we decrease P by k_i at each time $t_i \in (\tau_P, \tau_P + \tau_Q)$ such that $u(t_i) = \theta$, and similarly for Q when $v(t_i) = \theta$ for $t_i \in (0, \tau_P)$.

For a model that satisfies the assumptions given above, including (A0)–(A3), for fixed parameter values, we expect the main results obtained for the integrate and fire model to hold for the more general model, with similar justification to the analysis presented in this paper.